Chemical Science

Accepted Manuscript

This article can be cited before page numbers have been issued, to do this please use: C. Miesch, E. Krolicka, R. Mayer and D. Leboeuf, *Chem. Sci.*, 2026, DOI: 10.1039/D6SC03645G.




ROYAL SOCIETY OF CHEMISTRY

rsc.li/chemical-science

View Article Online
DOI: 10.1039/D6SC03645G

ARTICLE

# Switchable Reactivity of Homopropargylic Alcohols Towards γ-Arylated Ketones and α-Arylated Tetrahydrofurans in HFIP

Received 00th January 20xx,
Accepted 00th January 20xx

DOI: 10.1039/x0xx00000x

Claire Miesch,[a] Ewelina Krolicka,[a] Robert J. Mayer*[b] and David Lebœuf*[a]

A divergent synthetic strategy to access γ-arylated ketones and α-arylated tetrahydrofurans from readily available homopropargylic alcohols and arene nucleophiles is reported. This method expands the accessible chemical space of γ-arylated ketones via a unique triflic acid-catalyzed hydroalkoxylation/ring-opening arylation sequence proceeding through a 2,3-dihydrofuran intermediate, enabled by the properties of 1,1,1,3,3,3-hexafluoroisopropan-2-ol (HFIP) as solvent. This protocol provides a solution for preparing γ-arylated ketones incorporating sterically hindered arenes, while displaying compatibility with synthetically relevant functionalities to deliver linear and branched γ-arylated ketones, including both aliphatic and aromatic variants. Switching the reaction pathway by employing *p*-cymene as a hydride donor promotes a reductive hydroalkoxylation, affording α-arylated tetrahydrofurans with high efficiency. Mechanistic studies supported by DFT computations reveal a complex catalytic reaction network in which multiple pathways converge to the observed products.

## Introduction

Aryl-substituted aliphatic ketones are prevalent structural motifs in natural products, pharmaceuticals, materials, and agrochemicals. However, their utility goes beyond those applications as ketones represent pivotal functional groups in organic synthesis to install a large range of relevant functionalities into target molecules via their electrophilic *ipso* carbon and acidic α-C–H bonds, including amines, alcohols, alkenes, and esters, among others.[1,2] While manifold α- and β-arylations of ketones have been developed,[3-8] γ-arylation processes are largely underdeveloped because of the inherent difficulty in controlling their regioselectivity. In the past years, various disconnection strategies have emerged to address this issue, including elegant transition metal-catalyzed C–C cleavage of cyclobutanols,[9-13] cross-coupling reactions,[14-22] isomerization-based processes,[23-27] and C–H activation (Scheme 1).[28-30] Despite these advances, the synthesis of γ-arylated ketones incorporating sterically hindered arenes has still rarely been tackled.[12] Besides, the reaction design of these methods rarely provides access to both linear and branched γ-arylated ketones, while only delivering either aliphatic or aromatic ketones, for which synthetically useful electron-deficient aryl substitution patterns are underrepresented. Moreover, practical considerations for such protocols include the cost of transition-metal catalysts/ligands/additives used, their atom economy, and the removal of any trace metals for pharmaceutical applications. Therefore, metal-free and atom-economic access to distinct γ-arylated ketone architectures that are not readily attainable by existing disconnections would unlock underexplored chemical space.

Here, we envisioned a conceptually distinct approach to prior work, featuring readily available homopropargylic alcohols and non-pre-activated arenes as precursors. Specifically, our design plan starts with the intramolecular hydroalkoxylation of the alkyne to form a 2,3-dihydrofuran intermediate, which would then undergo a regioselective ring-opening intermolecular arylation with a sterically congested aryl C–H partner at the most accessible site to selectively afford the target γ-arylated ketones. In this strategy, the alcohol functionality plays two roles, acting as both an oxygen source to introduce the ketone into the final product and an electrophile to install the arene group. However, two potential pitfalls were identified: (**i**) the hydroalkoxylation of highly electronically deactivated alkynes, which were part of our coveted substrates, has rarely been observed, e.g., with gold catalysts,[31,32] and (**ii**) the ring-opening arylation of 2,3-dihydrofurans has only been described for π-activated substrates.[33] On the basis of our recent studies on the reactivity of deactivated alkynes/epoxides and aliphatic alcohols,[34-36] we hypothesized that employing 1,1,1,3,3,3-hexafluoroisopropan-2-ol (HFIP)[37-43] as a solvent in combination with a Brønsted acid may address those issues. HFIP would fulfill a dual role, amplifying, through its strong H-bond donating ability,[44,45] both the acidity of the catalyst to leverage the initial hydroalkoxylation step by protonation of the alkyne[34] and the electrophilicity of the 2,3-dihydrofuran intermediate to execute the ring-opening arylation with arene nucleophiles.[35]

[a] Laboratoire d'Innovation Moléculaire et Applications (LIMA) CNRS UMR 7042, Université de Strasbourg, Université de Haute-Alsace, 25 rue Becquerel, 67000 Strasbourg, France.
[b] Technical University of Munich, School of Natural Sciences, Department Chemie, 85748 Garching, Germany.

View Article Online DOI: 10.1039/D5SC03645G

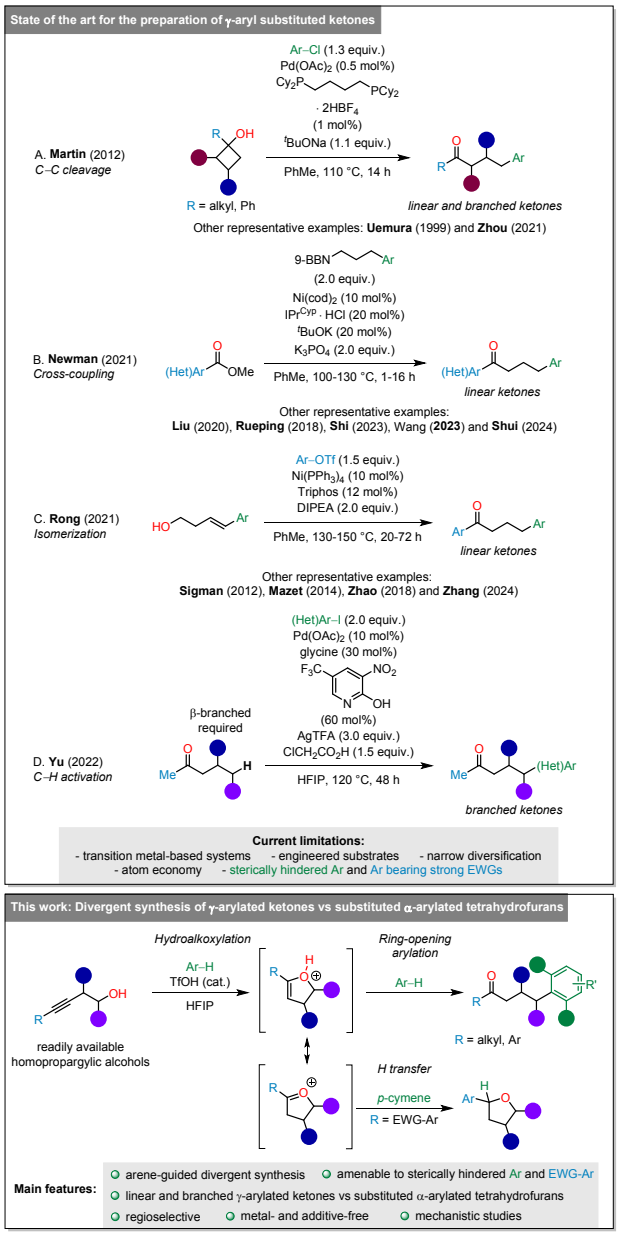


**Scheme 1** Synthetic approaches for the synthesis of γ-arylated ketones and divergent synthesis of substituted tetrahydrofurans from homopropargylic alcohols.

Herein, we report an operationally simple and atom-economic protocol to grant straightforward access to γ-arylated ketones from readily available homopropargylic alcohols and arenes, relying on a Brønsted acid-catalyzed reaction sequence in HFIP. The transformation enables the regioselective and stereospecific introduction of sterically hindered arenes and is compatible with alkynes bearing both electron-deficient and electron-rich aryl as well as alkyl substituents, while providing access to linear, β- and γ-branched ketones. Further, the use of inexpensive *p*-cymene as a biosourced H-donor[46] redirects the reaction pathway, providing direct access to α-arylated tetrahydrofurans, including polysubstituted ones that incorporate electron-deficient aryl groups. This unprecedented approach thereby offers a versatile platform for the divergent synthesis of compounds of interest. Further mechanistic experiments and DFT computations revealed a complex catalytic reaction network involved in product formation.

## Results and discussion

The initial optimization was performed on homopropargylic alcohol **1a**, employing mesitylene as an arene nucleophile (Table 1). After surveying various conditions, the highest yield for the target product **2** (90%) was obtained by conducting the reaction in HFIP (0.4 M) at 60 °C in the presence of 10 mol% of TfOH and an excess of mesitylene (5.0 equiv.) (Entry 1). Additional solvents were tested, but none delivered **2** with a yield exceeding 5% (Entries 2-7). In most cases, only the decomposition of **1a** was observed (Entries 2-5), underpinning the central role of HFIP in enabling the desired reactivity by presumably stabilizing reaction intermediates (see Table S1 in the Supporting Information for an optimization table with further information on the reaction outcome). In the same vein, replacing TfOH with other Lewis and Brønsted acids did not improve the yield of the reaction (Entries 8-18). The influence of other parameters, such as concentration, temperature, and the amount of mesitylene, was also examined, but did not lead to further improvement (Entries 19-23). Gratifyingly, we did not observe any significant decrease in yield by scaling up the reaction (5.0 mmol), as **2** was isolated in 85% yield (1.3 g).

**Table 1** Optimization studies for the formation of γ-arylated ketone **2**.

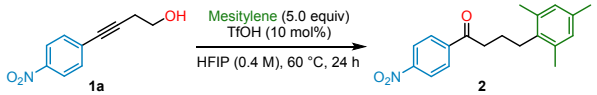


| Entry | Variation from standard conditions[a] | Yield[b] (%) |
|---|---|---|
| 1 | none | 90[c] |
| 2 | 1,2-DCE instead of HFIP | traces |
| 3 | 1,4-dioxane instead of HFIP | traces |
| 4 | Toluene instead of HFIP | traces |
| 5 | $MeNO_2$ instead of HFIP | traces |
| 6 | *i*PrOH instead of HFIP | NR |
| 7 | TFE instead of HFIP | 5 |
| 8 | HCl (37% aq.) instead of TfOH | traces |
| 9 | $H_2SO_4$ instead of TfOH | 82 |
| 10 | *p*TsOH·$H_2O$ instead of TfOH | 22 |
| 11 | CSA instead of TfOH | NR |
| 12 | $HNTf_2$ instead of TfOH | 50 |
| 13 | $Cu(OTf)_2$ instead of TfOH | 60 |
| 14 | $Bi(OTf)_3$ instead of TfOH | 78 |
| 15 | $Sc(OTf)_3$ instead of TfOH | 18 |
| 16 | $Yb(OTf)_3$ instead of TfOH | NR |
| 17 | $Al(OTf)_3$ instead of TfOH | 40 |
| 18 | $Ca(NTf_2)_2$/$nBu_4NPF_6$ instead of TfOH | traces |
| 19 | 0.2 M instead of 0.4 M | 77% |
| 20 | 0.6 M instead of 0.4 M | 76% |
| 21 | 80 °C instead of 60 °C | 89%[c] |
| 22 | 3.0 equiv. mesitylene instead of 5.0 equiv. | 82% |
| 23 | 1.0 equiv. mesitylene instead of 5.0 equiv. | 30% |

[a] Standard reaction conditions: homopropargylic alcohol **1a** (0.2 mmol, 1.0 equiv) and mesitylene (1.0 mmol, 5.0 equiv) in the presence of TfOH (10 mol%) in HFIP (0.4 M) at 60 °C for 24 h in a sealed pressure tube. [b] NMR yield using 1,3,5-trimethoxybenzene as an external standard. [c] Isolated yield.

With the established conditions in hand, the scope of the transformation was initially investigated with various sterically hindered arene nucleophiles (Scheme 2). As with mesitylene, the reaction with 1,3,5-triethylbenzene afforded the corresponding γ-arylated ketone **3** in 66% yield. Yet, for highly electron-rich 1,3,5-trimethoxybenzene, a prolonged reaction time (120 h) at 110 °C was required to obtain product **4** in 69% yield. This result might be attributed to the formation of an off-cycle species resulting from the protonation of the electron-rich arene in those highly acidic conditions,[47] a possible deactivation pathway for the reaction. We then evaluated the reactivity of various tri- and tetrasubstituted arenes decorated with an array of functional groups such as fluoride, bromide, methoxy, free OH, and phenyl. In our standard conditions, they provided a streamlined access to a variety of γ-arylated ketones in 30-97% yields (**5**-**17**). Of note, 1,3,5-trisubstituted arenes reacted with **1a** to form two regioisomers, which were separated by preparative thin-layer chromatography (TLC) (**6**-**9**, 30-88% combined yields). However, this issue was circumvented by introducing a bulkier substituent such as *tert*-butyl (**10**, 78%). The reaction was notably compatible with 1,1,4,4,6-pentamethyl-1,2,3,4-tetrahydronaphthalene, which is a key fragment of bexarotene (an antineoplastic agent), producing the corresponding compound **11** in 54% yield. Remarkably, product **2** could be re-engaged in the transformation as nucleophile to provide compound **17** in 68% yield. Pentasubstituted arenes were also compatible with the reaction to deliver, for instance, **18** in 78% yield. Lastly, we demonstrated that durene could undergo the reaction twice to afford γ-arylated diketone **19** in 50% yield.

Next, we examined the effect of the alkyne substitution pattern on the reactivity, using mesitylene as a model arene nucleophile. Highly electronically deactivated alkynes bearing synthetically useful electron-withdrawing groups (halide, $CF_3$, sulfonamide, $SO_2Me$, CN, $SCF_3$, ketone, ester, $OCF_3$, and amide groups) afforded the corresponding γ-arylated ketones in yields ranging from 38 to 95% (**20**-**35**), regardless of their position on the aryl ring (*ortho*, *meta*, and *para*). In the case of moderately electron-deficient and electron-rich aryl groups, such as 4-halophenyl, Ph, *p*Tol, and naphthalen-2-yl, the reaction also proceeded smoothly to provide the target compounds in 45-73% (**36**-**40**). Importantly, the reaction was not limited to the preparation of linear γ-arylated ketones but could also be extended to that of β- and γ-branched ketones, producing **41** and **42** in 70 and 65% yields, respectively. Further, we demonstrated the stereospecificity of the transformation by using *cis*-configured diastereoisomer **1y**, which exclusively led to *trans*-configured product **43** (61%) via stereoinversion. Here, the relative configuration of **43** was ascertained by NOESY NMR spectroscopy (see Supporting Information). Lastly, we tested the compatibility of our protocol with alkyl-substituted alkynes, which afforded aliphatic ketones **44**-**48** in 41-71% yields. Of note, in the case of chloro-substituted alkyl, increasing the temperature to 80 °C led to the additional substitution of chloride by mesitylene to deliver γ-diarylated ketone **48** in 82% yield. When using a strong electron-rich aryl alkyne, target product **49** was not observed, with the reaction forming γ-hydroxy ketone, indicating that the 2,3-dihydrofuran intermediate is likely not sufficiently electrophilic to undergo ring-opening arylation with mesitylene. Bulkier arenes such as 1,3,5-triisopropylbenzene only led to side reactions. In the case of 2-phenylindole, no reaction took place, and substrate **1a** remained intact. In the reaction conditions, the indole is likely protonated and, in contrast to 1,3,5-trimethoxybenzene, no turnover occurred. The same applied to thiophene. Di-/mono-substituted arenes such as *p*-xylene and anisole were less effective, providing γ-arylated ketones in low yields (<15%, **52** and **53**) along with several unidentified by-products. In the case of anisole, our hypothesis is that the reaction is directly correlated to the steric hindrance displayed by the arene nucleophile, as we observed the formation of tetrahydrofuran **53'**, resulting from the addition at the C2 position of the putative 2,3-dihydrofuran intermediate. This compound is likely to re-react under our acidic conditions.

To follow up on our steric effect assumption, we hypothesized that revising the arene substitution pattern of the aryl alkyne moiety by increasing the steric hindrance at the *o*-positions would impede nucleophilic addition at the C2 position of the putative 2,3-dihydrofuran intermediate. The reaction was first tested using 2,6-disubstituted aryl substrate **1af** with mesitylene, which afforded **54** in nearly quantitative yield (95%). To our delight, γ-arylated ketones **55-57** were now exclusively obtained in 61-85% yields, using *p*-xylene, toluene, and anisole as nucleophiles. The reaction also proved compatible with naturally occurring thymol (**58**, 63%).

At this point, we envisioned three mechanistic pathways to account for the formation of γ-arylated ketones (Scheme 3A). They are expected to proceed through different reaction intermediates such as a 2,3-dihydrofuran via hydroalkoxylation - our initial hypothesis - (**path A**), a γ-hydroxy ketone via hydration (**path B**), and a cyclopropyl ketone via dehydration (**path C**),[47,48] all intermediates possibly interconverting with each other.

To gain insights into the reaction mechanism, notably the inferred involvement of a 2,3-dihydrofuran intermediate, we analyzed the crude mixture of the model reaction by $^1$H NMR spectroscopy, quenching it after a reaction time of 1 h through the addition of a saturated solution of $NaHCO_3$ (Scheme 3B). Here, in addition to **1a** and **2**, ketones **59** (an expected intermediate of **path B**) and **60** were formed. When both **59** and **60** were subjected to standard reaction conditions in the presence of mesitylene, the target product **2** was obtained in nearly quantitative yield (95%), indicating that the transformation proceeds via a convergent mechanistic pathway possibly involving these intermediates.

View Article Online
DOI: 10.1039/D6SC03645G





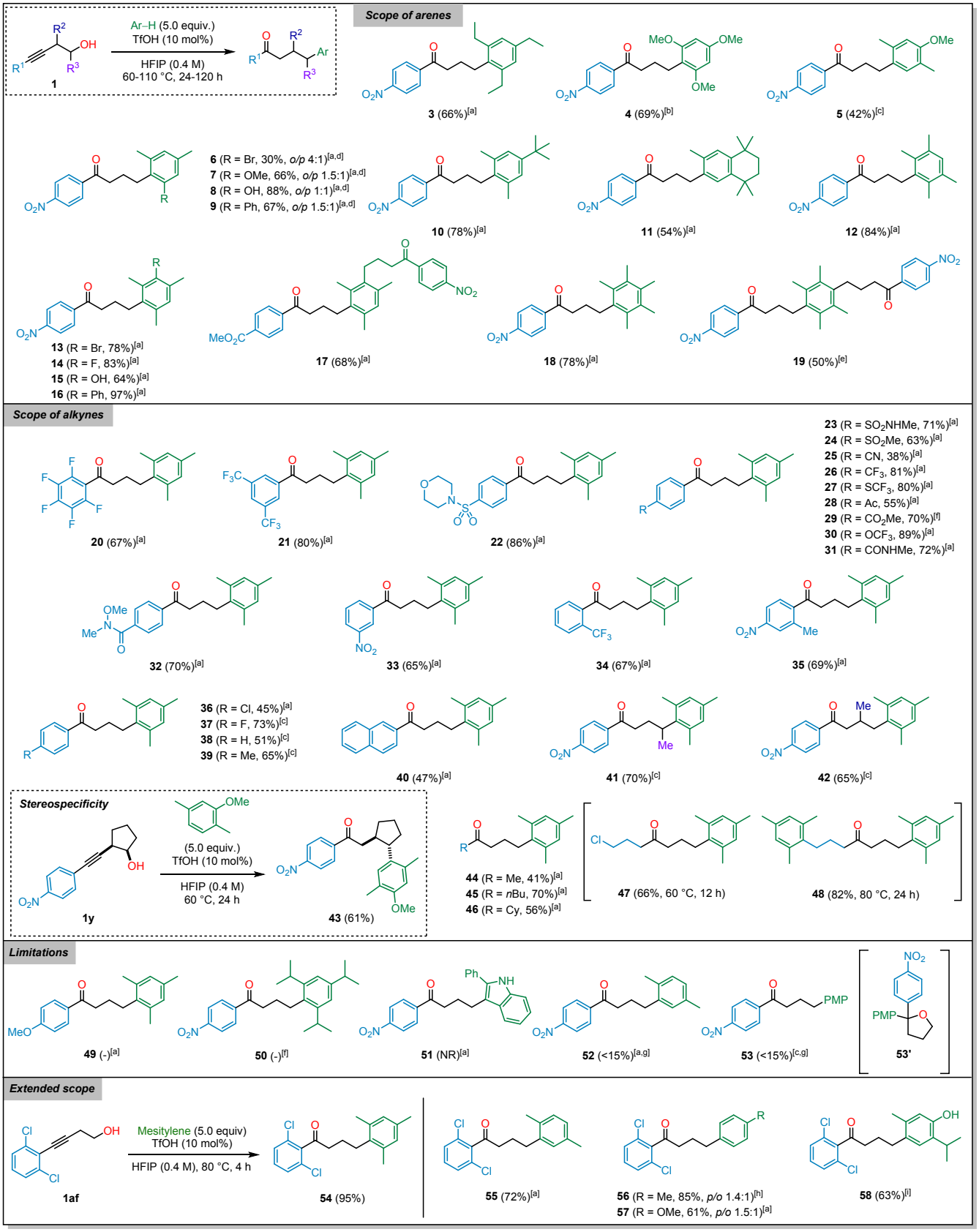


**Scheme 2.** Scope of γ-arylated ketones. [a] 80 °C, 24 h. [b] 110 °C, 120 h. [c] 110 °C, 24 h. [d] Regioisomers separable by preparative TLC. [e] 80 °C, 72 h. [f] 60 °C, 24 h. [g] NMR yield using 1,3,5-trimethoxybenzene as an external standard. [h] 80 °C, 48 h. [i] 80 °C, 4 h. PMP = 4-methoxyphenyl.

View Article Online
DOI: 10.1039/D6SC03645G



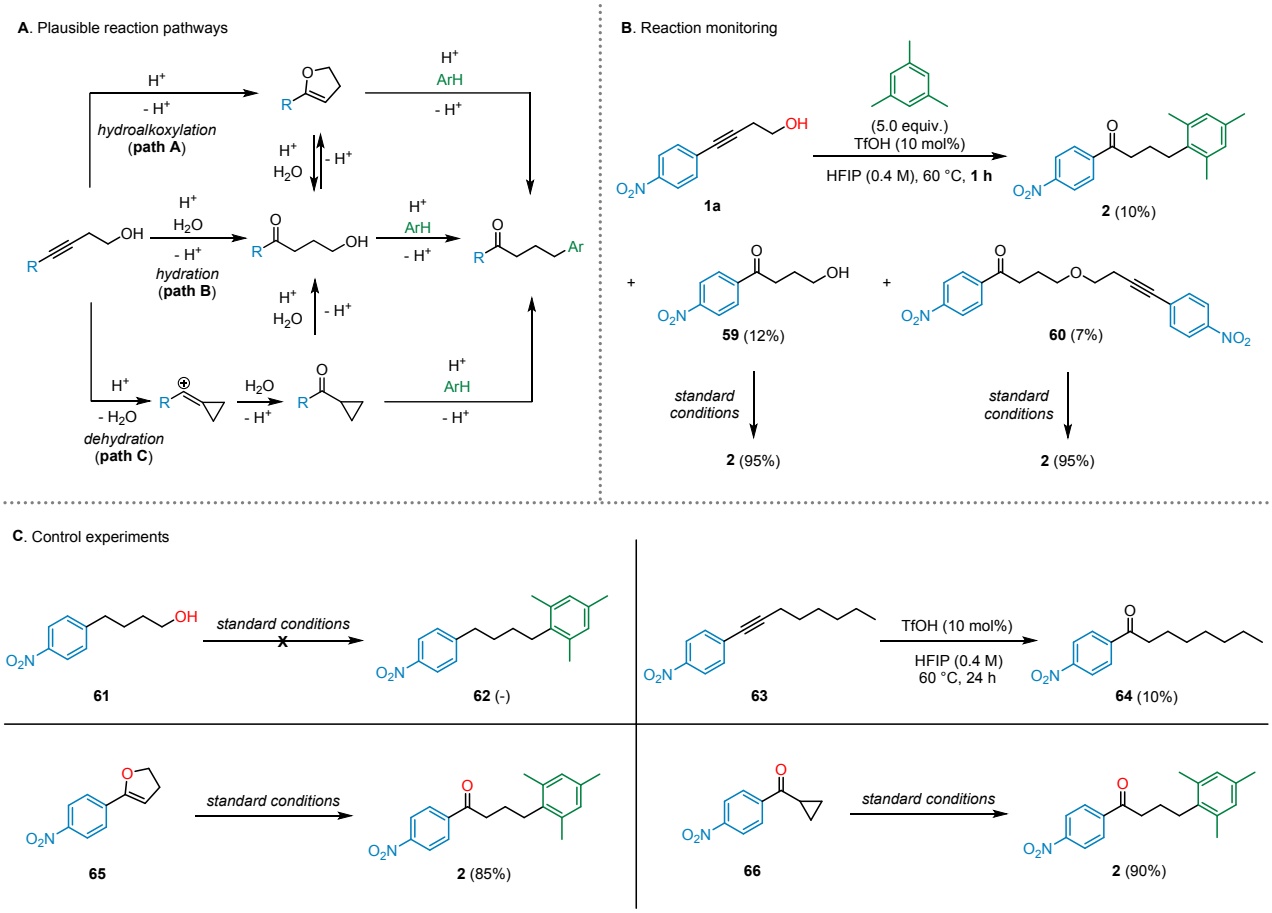


**Scheme 3** Control experiments regarding the mechanism of formation of γ-arylated ketones.

Next, we examined if the presence of the alkyne moiety was a prerequisite for the reaction since a direct arylation of the alcohol could be envisioned based on our previous report on the Friedel–Crafts arylation of primary aliphatic alcohols in HFIP (Scheme 3C).[35] However, alcohol **61** without the alkyne motif did not undergo the reaction. Since the hydration of alkynes to yield the corresponding ketones is well-established in acidic medium,[49-52] compound **63**, in which the alcohol functionality was absent, was also engaged in our standard conditions without mesitylene, providing ketone **64** in low yield (10%). Altogether, these results indicate that both functionalities are likely to act in synergy to provide **2**, corroborating our initial design proposal.

Although *in situ* monitoring of the reaction mixture by $^1$H NMR did not directly detect the postulated 2,3-dihydrofuran intermediate (**path A**), we assume that such a species is prone to react with any nucleophile present in the reaction medium. The same could be expected for a cyclopropyl aryl ketone intermediate (**path C**). Separately synthesized 2,3-dihydrofuran **65** and cyclopropyl aryl ketone **66**, subjected to the standard reaction conditions, delivered **2** in 85 and 90% yields, respectively (Scheme 3C), indicating the plausibility of both pathways, but preventing us from reaching a definitive conclusion at this point.

However, experimental support for our reaction design came serendipitously when we re-analyzed the reaction with 1,3,5-triisopropylbenzene as an arene nucleophile, yielding tetrahydrofuran **67** in 22% (Equation 1). This product likely arose from the reduction of 2,3-dihydrofuran intermediate **65**, 1,3,5-triisopropylbenzene serving as a H-donor in a reductive hydroalkoxylation process.[53,54]

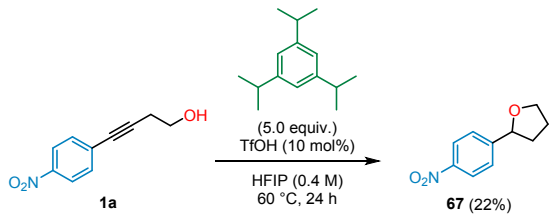


(1)

To elucidate the dominant reaction pathway leading to product formation, we performed quantum-chemical calculations to probe various potentially competing mechanisms (Scheme 4). The observed side products and control experiments guided our choice of investigated pathways (see Scheme 3). For each intermediate, we examined alternative routes by identifying the

View Article Online
DOI: 10.1039/D6SC03645G



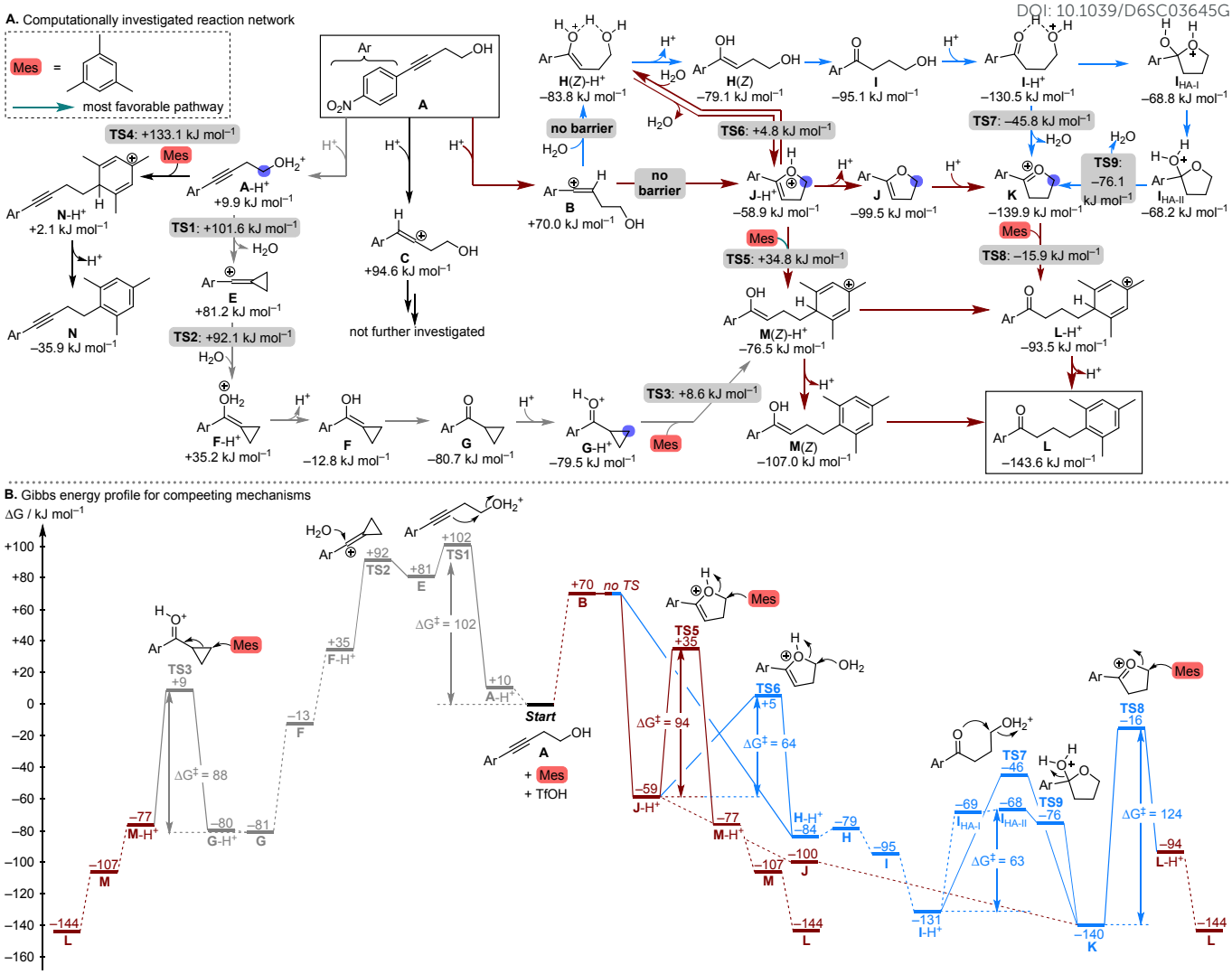


**Scheme 4** Computational analysis of the mechanistic pathways leading to product **L** starting through the TfOH-catalyzed reaction of **A** with mesitylene at the SMD(HFIP)/PWPB95-D4/def2-TZVPP//SMD(HFIP)/ωB97XD/def2-SVP level (the counterion for balancing protonated species is $TfO^-$; species were modeled as free species, not as ion pairs). (A) Reaction network with Gibbs energies for ground and transition states, and (B) Gibbs energy profile for the main pathways.

most reactive sites and the potential availability of water as a nucleophile (according to Karl Fischer titration, the employed HFIP contained 0.03% water, ca. 0.02 M) and TfOH as a proton source. All species were first subjected to a conformational search using Grimme's GFN2-xTB method.[55] The resulting geometries were then optimized at the SMD(HFIP)/ωB97-XD/def2-SVP and refined with single-point energies at the PWPB95-D4/def2-TZVPP levels,[56-58] adopting a previously employed protocol.[36]

The alcohol moiety represents the most basic site for protonation of **1a** (= **A**). Consistent with our experimental findings (Scheme 3C), direct nucleophilic substitution of water in **A**-$H^+$ by mesitylene to give the intermediate **N**-$H^+$ is kinetically disfavored ($\Delta G^‡$ = +133.1 kJ $mol^{-1}$). Instead, a viable route to product **2** (= **L**) that initiates with the protonation to **A**-$H^+$ proceeds via dehydration to form the cyclopropylidene cation **E**, followed by water addition (**F**–$H^+$), tautomerization to **G**, and intermolecular nucleophilic attack of mesitylene on the cyclopropyl aryl ketone **G**–$H^+$. The highest energy span in this sequence corresponds to the generation of cation **E** (+101.6 kJ $mol^{-1}$).[59]

The alkyne moiety is significantly less basic than the alcohol: the Gibbs energy for the protonation of **A** to give vinyl cations **B** and **C** is by 70.0 and 94.6 kJ $mol^{-1}$, respectively, less favorable than to yield **A**-$H^+$, equivalent to roughly 12 and 17 p$K_a$ units. We thus focused on possible sequences that emerge after formation of the more accessible intermediates **B** and **E** (unlike **C**), for which two main routes to product **L** emerge.

(**I**) Cyclization/ring-opening sequence (red pathway in Scheme 4): A barrierless intramolecular cyclization of **B** yields the aryl-dihydrofuranyl cation **J**–$H^+$. Ring-opening by mesitylene then proceeds with a barrier of +93.7 kJ $mol^{-1}$ to intermediate **M**(*Z*)-$H^+$, furnishing product **L** after proton transfer and tautomerization.

(**II**) Water trapping/cyclization/ring opening (blue pathway in Scheme 4): In the presence of sufficient amounts of water, **B** can undergo a nucleophilic attack by water to intermediate **H**(*Z*)-$H^+$

View Article Online
DOI: 10.1039/D6SC03645G



and tautomerize to ketone **43** (= **I**), which was observed experimentally. Protonation of the primary alcohol of **I** is highly favorable, triggering intramolecular attack on the carbonyl to form the cyclic oxonium ion **K**. Opening of **K** by mesitylene to afford the product scaffold proceeds through a barrier of +124 kJ mol$^{-1}$. Whereas the barrier for this last step corresponds to the highest barrier of the sequence, the barriers for the steps leading to **K** are lower than those of pathway (I).

Depending on the availability of water, the computed Gibbs energy profile does not conclusively favor either the blue or red route; instead, it suggests a catalytic reaction network converging on the thermodynamically most stable product through multiple pathways, each preferentially occurring under different reaction conditions. Both **H**–H$^+$ and **J**–H$^+$ are formed from **B** without a barrier, and, owing to the significant barriers for the reverse reaction (129 and 154 kJ mol$^1$, respectively), these steps are effectively irreversible. In *water-free* conditions, intramolecular cyclization with the terminal alcohol moiety is expected to dominate and to select the red pathway, whose largest energetic span is 94 kJ mol$^{-1}$. As a byproduct, **44** may form at this step due to trapping of **B** with **A**, yet we did not computationally consider this as a main pathway, as the effective molarity would likely favor the intramolecular cyclization. In the *presence of water*, however, the blue pathway is expected to prevail: even if **B** is not trapped directly, **J**–H$^+$ is more readily opened by water than by mesitylene ($\Delta G^‡$ = 64 vs. 94 kJ mol$^{-1}$), funneling flux into **I**–H$^+$ and onward through the blue sequence. Because the blue route's overall energetic span (+124 kJ mol$^{-1}$) exceeds that of the red route, increasing water content should proportionally slow the net conversion to product.

To our delight, those scenarios were confirmed experimentally. When drying the HFIP with 3Å molecular sieves, we exclusively observed the formation of product **2** by *in situ* $^1$H NMR, while ketones **59** and **60** were not detected. Yet, the addition of 5.0 equiv. of water to the reaction medium mostly precluded the formation of the target product **2** (yield ~ 10%), and instead led to the formation of ketone **59** (35%) as a major product (Equation 2). Under the preparative conditions employed in this study, the water content of the HFIP employed corresponds to approximately 0.1 equiv. (0.02 M water, see above), which is too little to slow the reaction down to the extent seen with 5.0 equiv.

Finally, we performed reactions with various amounts of water to evaluate how it affects the reactivity. We found that 0.5 and 1.0 equiv. had no impact on the reactivity, with NMR yields >95% for **2** after 24 h. The addition of 2.0 equiv. resulted, however, in a significant decrease in the reaction rate, yielding **2** in only 46% after 24 h. Those results clearly show that water is a parameter not to be overlooked when studying reactions in HFIP.

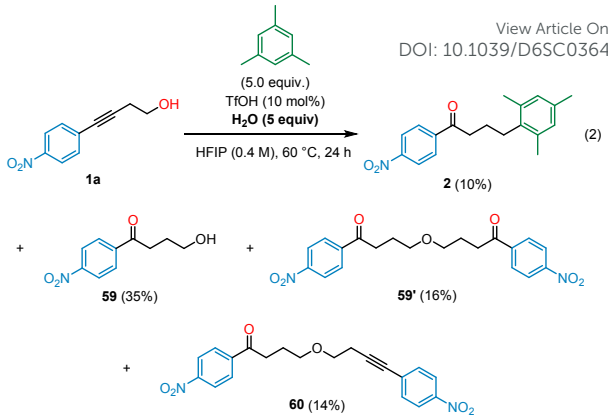


Based on the mechanistic insights obtained, we came to realize that this mechanistic scenario offers further synthetic opportunities as 5-aryl-4-pentyn-1-ol derivatives should deliver γ-arylated ketones, as a 5-*exo*-dig pathway should be favored over a 6-*endo*-dig one under acid catalysis. To test this hypothesis, we prepared substrate **68**, which gratifyingly led to the formation of **69** as a major product (62%) along with minor amounts of δ-arylated ketone **70** (18%) (Equation 3).

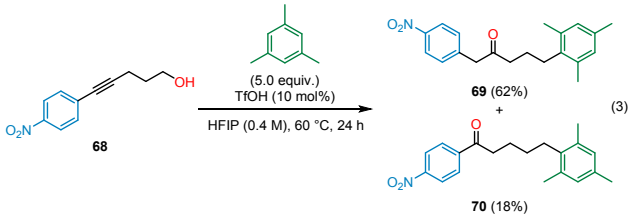


Intrigued by the switchable reactivity observed with 1,3,5-triisopropylbenzene (Equation 1), we turned our attention to the formation of α-arylated tetrahydrofurans, a structural motif found in several bioactive compounds.[60-62] A general method to access such scaffolds would give an additional benefit to our strategy by enabling divergent synthesis towards frameworks of interest from simple materials. Regarding aryl groups, electron-withdrawing substituents remain underexplored, prompting us to focus on this synthetic aspect. Currently, common strategies to access α-arylated tetrahydrofurans embedding electron-deficient aryl groups include α-arylation of tetrahydrofurans,[63-67] reduction of furans,[68,69] and hydroarylation of 2,3-dihydrofurans,[70,71] in which the 5-membered ring is already pre-constructed. However, when polysubstituted tetrahydrofurans are targeted, pre-installation of additional functional groups can be difficult, limiting the generality of those approaches. With respect to our preliminary findings, the reductive hydroalkoxylation of arylacetylenes has previously been described in the literature, using trimethylsilyl trifluoromethanesulfonate as a promoter (2.0 equiv.) in the presence of triethylsilane as hydride donor;[72] however, the reaction proved incompatible with aryl incorporating strong electron-withdrawing groups such as nitro.

Our search for the optimized conditions for accessing α-arylated tetrahydrofuran **67** led us to evaluate a large range of hydride donors (Table 2, Entries 1-7). Our screening revealed that the highest yield (98%) was obtained when *p*-cymene,

View Article Online
DOI: 10.1039/D5SC03145C

**Table 2** Optimization studies for the formation of α-arylated tetrahydrofuran **67**.

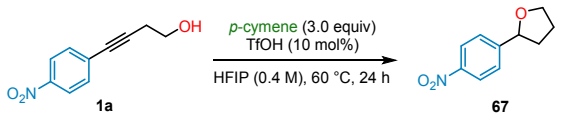


**1a** **67**

| Entry | Variation from standard conditions[a] | Yield[b] (%) |
|---|---|---|
| 1 | none | 98[c] |
| 2 | cumene instead of *p*-cymene | 38 |
| 3 | 1,4-diethylbenzene instead of *p*-cymene | 32 |
| 4 | 1,4-cyclohexadiene instead of *p*-cymene | 35 |
| 5 | γ-terpinene instead of *p*-cymene | 10 |
| 6 | triethylsilane instead of *p*-cymene | - |
| 7 | pinacolborane instead of *p*-cymene | 20 |
| 8 | Hantzsch ester instead of *p*-cymene | NR |
| 9 | $MeNO_2$ instead of HFIP | 16 |
| 10 | 1,2-DCE instead of HFIP | traces |
| 11 | Toluene instead of HFIP | traces |
| 12 | *i*PrOH instead of HFIP | NR |
| 13 | TFE instead of HFIP | 18 |
| 14 | 5.0 equiv. *p*-cymene instead of 3.0 equiv. | 68% |
| 15 | 1.0 equiv. *p*-cymene instead of 3.0 equiv. | 65% |

[a] Standard reaction conditions: homopropargylic alcohol **1a** (0.2 mmol, 1.0 equiv) and *p*-cymene (0.6 mmol, 3.0 equiv) in the presence of TfOH (10 mol%) in HFIP (0.4 M) at 60 °C for 24 h in a sealed pressure tube. [b] NMR yield using 1,3,5-trimethoxybenzene as an external standard. [c] Isolated yield.

which has a nucleophilicity parameter of −2.8 according to the Mayr database,[73] was used in HFIP with catalytic amounts of TfOH. Here, the key to the reaction's success is the moderate hydricity of *p*-cymene, so that the hydroalcoxylation step occurs before the reduction. When the reactivity was not matched, such as with triethylsilane, the target product **67** was not formed, and only the reduced alkyne was detected. As observed with the synthesis of γ-arylated ketones, employing HFIP as a solvent is crucial, as other solvents failed to produce **67** in a satisfactory yield (Entries 8-12). Additionally, the reaction was achieved on a larger scale (5.0 mmol) to deliver **67** in 80% yield (0.77 g).

We then examined the scope of this reaction. Electronically deactivated alkynes adorned with privileged synthetic functionalities afforded the corresponding α-arylated tetrahydrofurans in yields ranging from 33 to 90% (**71**-**85**) (Scheme 5). The transformation also proved compatible with the formation of polysubstituted tetrahydrofurans (**87**-**90**, 44-96%). Remarkably, in the case of octahydrobenzofuran **90**, whose structure was ascertained by NOESY NMR spectroscopy, the reaction operates under complete diastereocontrol. Not surprisingly, using a substrate hindered at both *ortho*-positions precluded the desired reactivity. By analogy to the arylation protocol described above, 5-aryl-4-pentyn-1-ols were also compatible with this transformation, affording tetrahydrofuran product **91** in 83% yield. In contrast, in the case of electron-neutral and -rich arenes ($R^1$ = Ph, *p*Tol, and PMP), we only obtained γ-hydroxy ketones, which proved not competent intermediates to afford the target α-arylated tetrahydrofurans (see Scheme 6A).

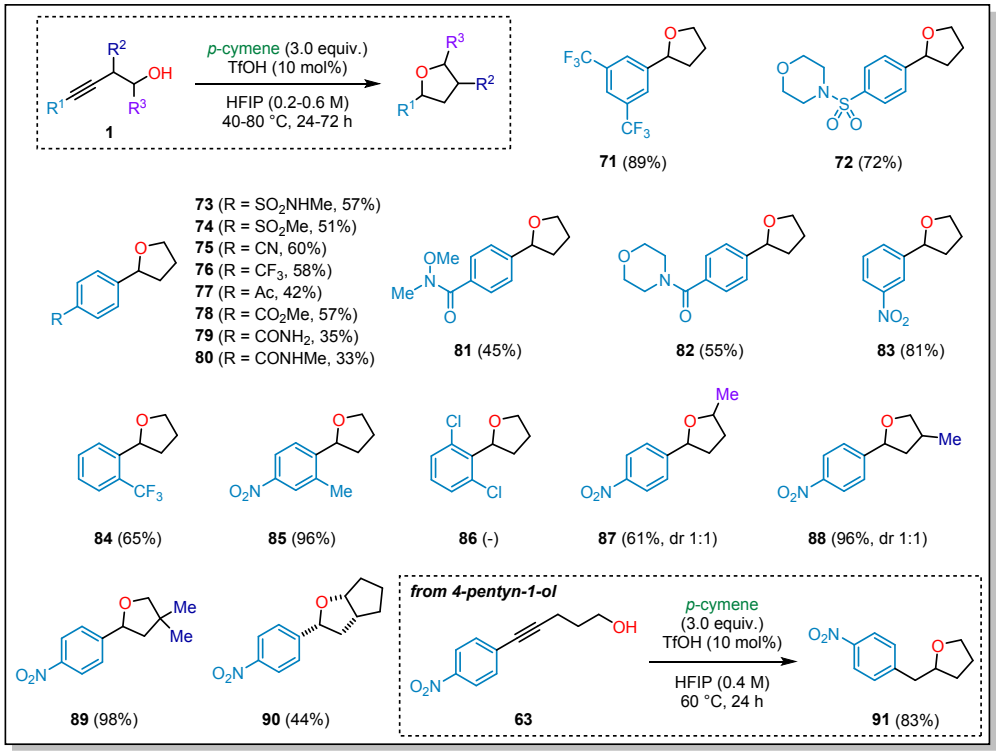


**Scheme 5** Scope of α-arylated tetrahydrofurans.

Next, we conducted several experiments to provide some insight into the reaction mechanism of the reductive hydroalcoxylation of homopropargylic alcohols (Scheme 6). We commenced by evaluating the reactivity of several potential intermediates, such as 2,3-dihydrofuran **65**, γ-hydroxy ketone **59**, and homoallylic alcohol **92**, in our standard conditions. Here, only the reaction with **65** led to the formation of α-arylated tetrahydrofuran **67** in 90% yield, suggesting its intermediacy in the reaction. Then, to assess the origin of hydrogens at the C2 and C3 positions of **67**, we performed reactions with deuterated HFIP and *p*-cymene. HFIP-D1 efficiently incorporated deuterium into product **67a-D** (100%D) at C3, which is consistent with the initial protonation proposed for the formation of γ-arylated ketones (see Scheme 5). This result might be explained by a fast proton exchange between TfOH and HFIP.[74] In the case of *p*-cymene-D, deuterium was nearly fully introduced at C2 to yield **67b-D** (90%D), indicating that *p*-cymene acts as a hydride donor via its methine group. This finding was confirmed by performing the reaction with an excess of alcohol **1a** (2.0 equiv.), which led to the complete consumption of *p*-cymene to generate indane *93* (95%). This product likely arose from the reaction between a *p*-cumyl cation and *p*-isopropenyltoluene, as previously observed in studies on H-transfer involving *p*-cymene.[75]

Experiments provide evidence that species **67** is formed via nucleophilic hydride transfer to the intermediate **K**. We therefore also evaluated this possibility using quantum-chemical calculations (Scheme 7). The hydride transfer of *p*-cymene to **K** is computed to proceed through a barrier of +75.9 kJ mol$^{-1}$, which is significantly lower than the barrier for the addition as a carbon-nucleophile (+124 kJ mol$^{-1}$ in the case of mesitylene, cf. Scheme 4). However, the formation of the tetrahydrofuran **67** alongside the corresponding tertiary carbenium ion is computed to be endergonic with a reaction energy of ΔG0 = +40.0 kJ mol$^{-1}$ and thus reversible. Considering the formation of indane **93** as the final reaction product, the reaction becomes more favourable with an energy of $\Delta G^0$ = +13.1 kJ mol$^{-1}$; this value is further reduced to $\Delta G^0$ = –2.4 kJ mol$^{-1}$ when explicit solvation of both $TfO^-$ and TfOH by one molecule of HFIP is considered. Given the experimental findings that **93** is the sole product, the computations likely overestimate the reaction energy, presumably due to insufficient description of specific solute-solvent interactions, yet support that hydride transfer to an oxocarbenium ion is a kinetically viable pathway. Notably, when the thermochemistry for the reduction of **K** by *p*-cymene is evaluated with a *p*-OMe instead of a *p*-$NO_2$ group in the computations, the reaction becomes highly endergonic (+115.4 kJ mol$^{-1}$), providing an explanation for the necessity of acceptor-substituents for forming tetrahydrofurans.

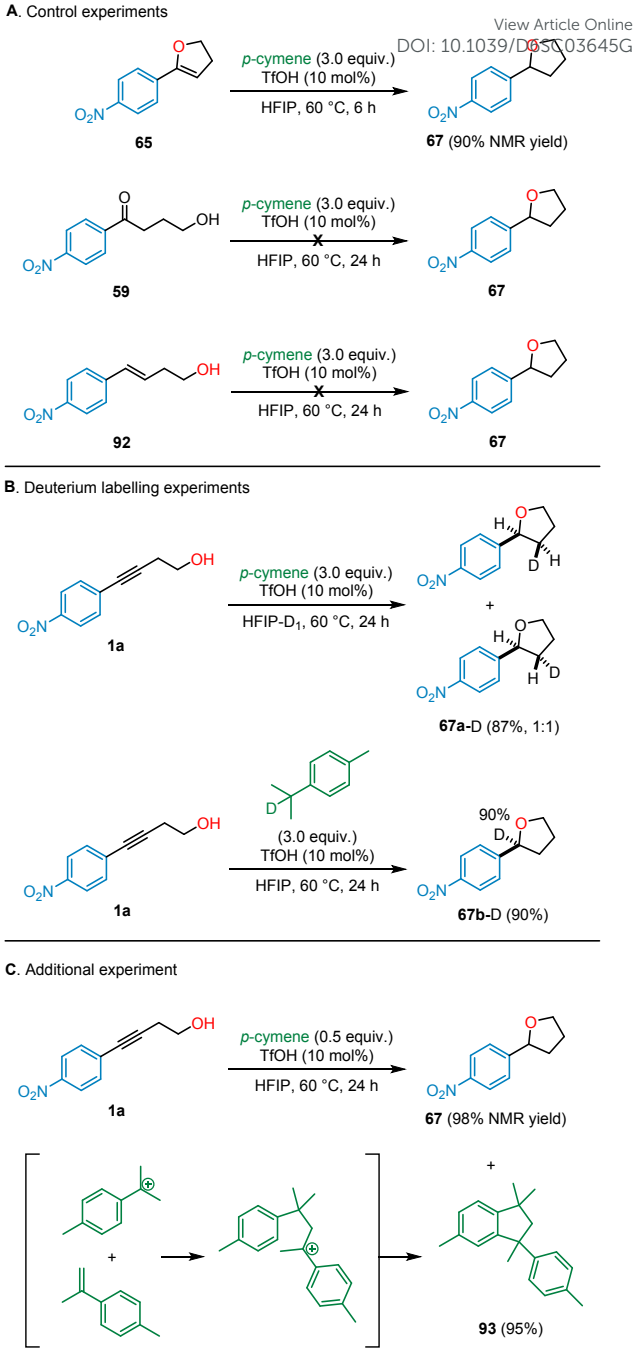


**Scheme 6** Mechanistic experiments regarding the formation of α-arylated tetrahydrofurans.

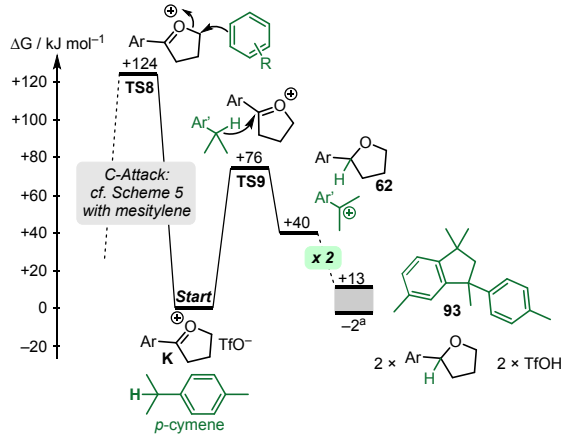


**Scheme 7** Computational analysis of hydride transfer from *p*-cymene + **K**. The overall reaction energy for the formation of indane **93** is calculated relative to 2 x (**K**, $TfO^-$, *p*-cymene) as the reactants. [a] Considering the explicit solvation of $TfO^-$ and TfOH by HFIP.

## Conclusions

In summary, we devised a strategy to provide modular access to γ-arylated ketones and α-arylated tetrahydrofurans from readily available homopropargylic alcohols and arenes. This method relies on a hydroalkoxylation/ring-opening arylation (hydride transfer) sequence, in which the combination of TfOH and HFIP is crucial for achieving the desired transformation. This approach enables the preparation of both linear and branched γ-arylated ketones incorporating sterically hindered arenes, while being compatible with alkyl- and aryl-substituted alkynes bearing an array of synthetically useful functionalities. Its simplicity, scalability, and atom economy further highlight the synthetic utility of this protocol. Further, using *p*-cymene as a hydride donor promotes access to a series of α-arylated tetrahydrofurans, including polysubstituted ones, which embed a large range of synthetically relevant functional groups, while bypassing the use of more expensive hydride donor sources such as silanes, boranes, or Hantzsch esters. Finally, a combination of mechanistic experiments and DFT calculations revealed the most likely reaction pathways that account for the observed reactivity. We anticipate that the method described will provide an entry point for utilizing the reactivity of aliphatic alcohols towards applications in the fine chemicals industry, with the ability to functionalize new C–O bonds.

## Author contributions

D.L. conceptualized this work and designed the experiments. C.M. and E.K. performed the experiments and analyzed the data. R.J.M. performed and analyzed the DFT calculations for the mechanistic investigation. R.J.M and D.L. drafted, reviewed, and edited the manuscript.

## Conflicts of interest

There are no conflicts to declare.

## Data availability

View Article Online
DOI: 10.1039/D6SC03645G

The data supporting this article have been included as part of the Supplementary Information.

## Acknowledgements

R.J.M. thanks the Deutsche Forschungsgemeinschaft (DFG, German Research Foundation) for support within the Emmy Noether Program (DFG, MA 9687/3-1, project number 553844165). D. L. thanks the ANR (ANR-23-CE07-0050-01), the CNRS, and the Université of Strasbourg for their support.

## Notes and references

1 J. Otera (ed.), *Modern Carbonyl Chemistry*, Wiley-VCH, Weinheim, 2000.
2 D. J. Foley and H. Waldmann, *Chem. Soc. Rev.*, 2022, **51**, 4094–4120.
3 T. Hayashi and K. Yamasaki, *Chem. Rev.*, 2003, **103**, 2829–2844.
4 C. C. C. Johansson and T. J. Colacot, *Angew. Chem. Int. Ed.*, 2010, **49**, 676–707.
5 F. Bellina and R. Rossi, *Chem. Rev.*, 2010, **110**, 1082–1146.
6 Z. Huang and G. Dong, *Tetrahedron Lett.*, 2014, **55**, 5869–5889.
7 Y.-J. Hao, X.-S. Hu, Y. Zhou, J. Zhou and J.-S. Yu, *ACS Catal.*, 2020, **10**, 955–993.
8 C. Wang and G. Dong, *ACS Catal.*, 2020, **10**, 6058–6070.
9 T. Nishimura and S. Uemura, *J. Am. Chem. Soc.*, 1999, **121**, 11010–11011.
10 T. Nishimura, S. Matsumura, Y. Maeda and S. Uemura, *Chem. Commun.*, 2002, 50–51.
11 S. Matsumura, Y. Maeda, T. Nishimura and S. Uemura, *J. Am. Chem. Soc.*, 2003, **125**, 8862–8869.
12 A. Ziadi and R. Martin, *Org. Lett.*, 2012, **14**, 1266–1269.
13 Z. Wang, Y. Hu, H. Jin, Y. Liu and B. Zhou, *J. Org. Chem.*, 2021, **86**, 466–474.
14 X. Liu, C.-C. Hsiao, L. Guo and M. Rueping, *Org. Lett.*, 2018, **20**, 2976–2979.
15 J. Masson-Makdissi, J. K. Vandavasi and S. G. Newman, *Org. Lett.*, 2018, **20**, 4094–4098.
16 A. Chatupheeraphat, H.-H. Liao, W. Srimontree, L. Guo, Y. Minenkov, A. Poater, L. Cavallo and M. Rueping, *J. Am. Chem. Soc.*, 2018, **140**, 3724–3735.
17 W. Sun, L. Wang, Y. Hu, X. Wu, C. Xia and C. Liu, *Nat. Commun.*, 2020, **11**, 3113.
18 Y.-L. Zheng, P.-P. Xie, O. Daneshfar, K. N. Houk, X. Hong and S. G. Newman, *Angew. Chem. Int. Ed.*, 2021, **60**, 13476–13483.
19 H. Chen, H. Yue, C. Zhu and M. Rueping, *Angew. Chem. Int. Ed.*, 2022, **61**, e202204144.
20 J. Ni, X. Xia, D. Gu and Z. Wang, *J. Am. Chem. Soc.*, 2023, **145**, 14884–14893.
21 J. Wang, Y. Yin, X. He, Q.-L. Duan, R. Bai, H.-W. Shi and R. Shi, *ACS Catal.*, 2023, **13**, 8161–8168.
22 X.-B. Yan, N. Wang, J. Zhou, H. Ge, Z. Wang, Y. Lin and H. Shui, *Org. Lett.*, 2024, **26**, 6518–6522.
23 E. W. Werner, T. Mei, A. J. Burckle and M. S. Sigman, *Science*, 2012, **338**, 1455–1458.
24 E. Larionov, L. Lin, L. Guénée and C. Mazet, *J. Am. Chem. Soc.*, 2014, **136**, 16882–16894.
25 R.-Z. Huang, K. K. Lau, Z. Li, T.-L. Liu and Y. Zhao, *J. Am. Chem. Soc.*, 2018, **140**, 14647–14654.

26 X. Wang, F. Liu, Z. Yan, Q. Qiang, W. Huang and Z.-Q. Rong, *ACS Catal.*, 2021, **11**, 7319–7326.
27 J.-W. Song, F. Xia, X.-L. Zhang and C.-P. Zhang, *Org. Chem. Front.*, 2024, **11**, 4219–4230.
28 R.-Y. Zhu, Z.-Q. Li, H. S. Park, C. H. Senanayake and J.-Q. Yu, *J. Am. Chem. Soc.*, 2018, **140**, 3564–3568.
29 Y.-H. Li, Y. Ouyang, N. Chekshin and J.-Q. Yu, *ACS Catal.*, 2022, **12**, 10581–10586.
30 K. Jia, J. Luo and C. Jiang, *Asian J. Org. Chem.*, 2025, **14**, e202500289.
31 A. Zhdanko and M. E. Maier, *Chem. Eur. J.*, 2014, **20**, 1918–1930.
32 R. Galéa and G. Blond, *Adv. Synth. Catal.*, 2022, **364**, 1532–1536.
33 K. Huang, H. Wang, L. Liu, W. Chang and J. Li, *Chem. Eur. J.*, 2016, **22**, 6458–6465.
34 S. Wang, G. Force, J.-F. Carpentier, Y. Sarazin, C. Bour, V. Gandon and D. Lebœuf, *Org. Lett.*, 2021, **23**, 2565–2571.
35 S. Zhang, M. Vayer, F. Noël, V. D. Vuković, A. Golushko, N. Rezajooei, C. N. Rowley, D. Lebœuf and J. Moran, *Chem*, 2021, **7**, 3425–3441.
36 M. Van Hoof, R. J. Mayer, J. Moran and D. Lebœuf, *Angew. Chem. Int. Ed.*, 2025, **64**, e202417089.
37 I. Colomer, A. E. R. Chamberlain, M. B. Haughey and T. J. Donohoe, *Nat. Rev. Chem.*, 2017, **1**, 0088.
38 V. Pozhydaiev, M. Power, V. Gandon, J. Moran and D. Lebœuf, *Chem. Commun.*, 2020, **56**, 11548–11564.
39 T. Bhattacharya, A. Ghosh and D. Maiti, *Chem. Sci.*, 2021, **12**, 3857–3870.
40 H. F. Motiwala, A. M. Armaly, J. G. Cacioppo, T. C. Coombs, K. R. K. Koehn, V. M. Norwood IV and J. Aubé, *Chem. Rev.*, 2022, **122**, 12544–12747.
41 M. Piejko, J. Moran and D. Lebœuf, *ACS Org. Inorg. Au*, 2024, **4**, 287–300.
42 S. Ghosh, K. Patra and M. Baidya, *Eur. J. Org. Chem.*, 2024, **27**, e202301321.
43 X. Xy, H. Luo and H. Gao, *Tetrahedron Green Chem.*, 2025, **5**, 100071.
44 A. Berkessel, J. A. Adrio, D. Hüttenhain and J. M. Neudörfl, *J. Am. Chem. Soc.*, 2006, **128**, 8421–8426.
45 A. Berkessel and J. A. Adrio, *J. Am. Chem. Soc.*, 2006, **128**, 13412–13420.
46 A. Balahbib, N. El Omari, N. El Hachlafi, F. Lakhdar, N. El Menyiy, N. Salhi, H. N. Mrabti, S. Bakrim, G. Zengin and A. Bouyahya, *Food Chem. Toxicol.*, 2021, **153**, 112259.
47 E. Richmond, J. Yi, V. D. Vuković, F. Sajadi, C. N. Rowley and J. Moran, *Chem. Sci.*, 2018, **9**, 6411–6416.
48 E. Richmond, V. D. Vuković and J. Moran, *Org. Lett.*, 2018, **20**, 574–577.
49 N. Menashe and Y. Shvo, *J. Org. Chem.*, 1993, **58**, 7434–7439.
50 T. Tsuchimoto, T. Joya, E. Shirakawa and Y. Kawakami, *Synlett*, 2000, 1777–1778.
51 S. Liang, G. B. Hammond and B. Xu, *Chem. Commun.*, 2015, **51**, 903–906.
52 W. Liu, H. Wang and C.-J. Li, *Org. Lett.*, 2016, **18**, 2184–2187.
53 L. R. C. Barclay, J. W. Hilchie, A. H. Gray and N. D. Hall, *Can. J. Chem.*, 1960, **38**, 94–103.
54 K. Bevernaegen, N. V. Tzouras, A. Poater, L. Cavallo, S. P. Nolan, F. Nahra and J. M. Winne, *Chem. Sci.*, 2023, **14**, 9787–9794.
55 C. Bannwarth, S. Ehlert and S. Grimme, *J. Chem. Theory Comput.*, 2019, **15**, 1652–1671.
56 A. V. Marenich, C. J. Cramer and D. G. Truhlar, *J. Phys. Chem. B*, 2009, **113**, 6378–6396.
57 J.-D. Chai and M. Head-Gordon, *Phys. Chem. Chem. Phys.*, 2008, **10**, 6615–6620.
58 F. Neese, *WIREs Comput. Mol. Sci.*, 2025, **15**, e70019.
59 S. Kozuch and S. Shaik, *Acc. Chem. Res.*, 2011, **44**, 101–110.
60 A. D. Rodríguez, O. M. Cóbar and O. L. Padilla, *J. Nat. Prod.*, 1997, **60**, 915–917.
61 A. T. Maioli, R. L. Civiello, B. M. Foxman and D. M. Gordon, *J. Org. Chem.*, 1997, **62**, 7413–7417.
62 F. Bennett, A. K. Saksena, R. G. Lovey, Y. T. Liu, N. M. Patel,P. Pinto, R. Pike, E. Jao, V. M. Girijavallabhan, A. K. Ganguly,D. Loebenberg, H. Wang, A. Cacciapuoti, E. Moss, F. Menzel,R. S. Hare and A. Nomeir, *Bioorg. Med. Chem. Lett.*, 2006, **16**, 186–190.
63 D. R. Heitz, J. C. Tellis and G. A. Molander, *J. Am. Chem. Soc.*, 2016, **138**, 12715–12718.
64 B. J. Shields and A. G. Doyle, *J. Am. Chem. Soc.*, 2016, **138**, 12719–12722.
65 Y. Shen, Y. Gu and R. Martin, *J. Am. Chem. Soc.*, 2018, **140**, 12200–12209.
66 Y. Gong, L. Su, Z. Zhu, Y. Ye and H. Gong, *Angew. Chem. Int. Ed.*, 2022, **61**, e202201662.
67 S. Xu, Y. Ping, W. Li, H. Guo, Y. Su, Z. Li, M. Wang and W. Kong, *J. Am. Chem. Soc.*, 2023, **145**, 5231–5241.
68 J. Wysocki, N. Ortega and F. Glorius, *Angew. Chem. Int. Ed.*, 2014, **53**, 8751–8755.
69 N. Frank, M. Leutzsch and B. List, *J. Am. Chem. Soc.*, 2025, **147**, 7932–7938.
70 D. Rosas Vargas and S. P. Cook, *Tetrahedron*, 2018, **74**, 3314–3317.
71 H.-K. Sun, X. Lu and Y. Fu, *ChemCatChem*, 2025, **17**, e202401610.
72 S. J. Gharpure, D. S. Vishwakarma and S. K. Nanda, *Org. Lett.*, 2017, **19**, 6534–6537.
73 M. Horn, L. H. Schappele, G. Lang-Wittkowski, H. Mayr and A. R. Ofial, *Chem. Eur. J.*, 2013, **19**, 249–263.
74 X. Zhou, J. Zhang, M. Sun, H.-Q. Yang, Z. Wang, J. Yang and G.-B. Huang, *J. Org. Chem.*, 2025, **90**, 2879–2888.
75 A. Elgavi and H. Pines, *J. Catal.*, 1978, **55**, 228–239.

View Article Online
DOI: 10.1039/D6SC03645G

The data supporting this article have been included as part of the Supplementary Information.